Nonlinear Three-Wave Interaction among Barotropic Rossby Waves in a Large-scale Forced Barotropic Flow

Luo Dehai (罗德海)

Department of Atmospheric and Oceanic Sciences, Ocean University of Qingdao, Qingdao 266003

(Received December 1, 1997; revised October 12, 1998)

ABSTRACT

In this paper, the coupling equations describing nonlinear three-wave interaction among Rossby waves including the forcing of an external vorticity source are obtained. Under certain conditions, the coupling equations with a constant amplitude forcing, the stability analysis indicates that when the amplitude of the external forcing increases to a certain extent, a pitchfork bifurcation occurs. Also, it is shown from numerical results that the bifurcation can lead to chaotic behavior of "strange" attractor. For the obtained three-variable equation, when the amplitude of modulated external forcing gradually increases, a period-doubling bifurcation is found to lead to chaotic behavior. Thus, in a nonlinear three-wave coupling model in the large-scale forced barotropic atmospheric flow, chaotic behavior can be observed. This chaotic behavior can explain in part 30-60-day low-frequency oscillations observed in mid-high latitudes.

Key words: Rossby waves, Three-wave interaction, 30-60-day low frequency oscillation

1. Introduction

Since nonlinear three-wave interaction among Rossby waves in the large-scale unforced barotropic flow was investigated by Longuet-Higgins et al. (1967), a considerable study on this aspect had been made (Loesch, 1974; Jones, 1979). Egger (1978), Cree and Swaters (1991) and Luo (1994) had extended nonlinear three-wave coupling among Rossby waves to include large-scale topographic forcing and attempted to explain the onset of atmospheric blocking situation and the appearance of 30-60-day oscillation. However, no chaos was found in all these studies.

Wersinger, Finn and Ott (1980a,b), Hughes and Proctor (1990a,b; 1992) had investigated in detail the non-conservative nonlinear three-wave mode coupling, and found that when one of the three wave modes is linearly unstable and the other two are linearly damped (they are assumed to possess the same damping rate), this model can be reduced to three-variable equations. In certain parameter ranges, chaos can be detected. However, in the atmospheric flow, all Rossby waves are usually damped. In this case, if the external forcing is not considered, chaos may not occur in the atmospheric three-wave mode coupling model, the external vorticity source forcing must be required.

In the present paper, we constuct a new chaotic model of three-wave mode coupling among Rossby waves in a large-scale forced flow, and give some numerical solutions. The main outline is as follows. In Section 2, the nonlinear equations describing nonlinear three-wave near-resonant interaction among Rossby waves in a large-scale forced barotropic flow are obtained. Under certain conditions, these equations can be reduced to four- and three-variable equations. In Section 3, for the constant amplitude forcing the

stability analysis of the four-variable equations without dissipation is made, and a pitchfork bifurcation is found. In addition, the numerical solutions of this system are given in this section, and chaotic solutions of "strange" attractor are found. In Section 4, we give the numerical solutions of the three-variable equations for a modulated external forcing, and the chaotic solutions of this system are found. In Section 5, the numerical solutions of the three-variable equations for a modulated external forcing and with a stronger dissipation are given. The conclusions are given in Section 6.

2. The forced barotropic model and nonlinear three-wave coupling equations

2.1 *The forced barotropic model*

The nondimensional barotropic vorticity equation of the large-scale barotropic flow with dissipation and external vorticity source on an infinite beta plane can be written in the form (Charney and Devore, 1979)

$$\frac{\partial}{\partial t}\nabla^2\psi + J(\psi,\nabla^2\psi) + \beta\frac{\partial\psi}{\partial x} = \nabla^2\psi^* - R_e\nabla^2\psi, \tag{1}$$

where ψ is the streamfunction, $\beta = \frac{L^2}{U}\beta_0$ and $\beta_0 = \frac{2\omega_0}{a_0}\cos\varphi_0$, ψ^* is the streamfunction of external vorticity source, and its coefficient has been combined into itself, R_e is the nondimensional friction coefficient and $R_e << 1.0$, $L = 10^6 m$ and $U = 10$ m/s are the characteristic horizontal length and velocity scales, respectively. The other notation can be found in Charney and Devore (1979). In this paper, for simplicity we assume that the external vorticity source is weaker so that $\psi^* = O(\varepsilon^2)$ is allowed like Luo (1994).

2.2 *The forced three-wave coupling equations*

In this subsection, based on the $\psi^* = O(\varepsilon^2)$ case, we assume $R_e = \varepsilon R_{e0}$ and $\psi^* = \varepsilon^2\psi_*$, where $\gamma_0 \leqslant \varepsilon << 1.0$ and $\gamma_0 = \frac{U}{f_* L} \approx 0.1$ is the local Rossby number. In this case, we introduce

$$T = \varepsilon t, \tag{2}$$

and expand ψ as

$$\psi = -\bar{u}y + \sum_{n=1}^{\infty}\varepsilon^n\psi_n(x,y,t,T), \tag{3}$$

where $\bar{u}$ is the zonal mean westerly wind and a constant.

Substituting (2) and (3) into (1), we obtain

$$O(\varepsilon^1): L(\psi_1) = (\frac{\partial}{\partial t} + \bar{u}\frac{\partial}{\partial x})\nabla^2(\psi_1) = \beta\frac{\partial(\psi_1)}{\partial x} = 0, \tag{4a}$$

$$O(\varepsilon^2): L(\psi_2) = -\frac{\partial}{\partial T}\nabla^2\psi_1 - J(\psi_1,\nabla^2\psi_1) - R_{e0}\nabla^2\psi_1 + \nabla^2\psi_*. \tag{4b}$$

Eq. (4a), being linear and not including any forcing, permits a solution consisting of the superposition of three Rossby waves in the form

$$\psi_1 = \sum_{n=1}^{3} A_n(T)e^{i\theta_n} + cc \tag{5}$$

where $\theta_n = k_n x + m_n y - \omega_n t (n = 1,2,3)$, k_n and m_n are the zonal and meridional wavenumbers of the nth Rossby wave respectively, $\omega_n = \bar{u}k_n - \dfrac{\beta k_n}{k_n^2 + m_n^2}$ is the frequency of the nth Rossby wave, $A_n(T)$ denotes the complex amplitude of the nth Rossby wave, and cc the conjugate of its preceeding terms.

In the Northern Hemispheric mid–high latitudes, the external vorticity source usually has the "zonal wavenumbers 2–3" structure. Here, the prescribed external vorticity source is assumed to be of the form

$$\psi_e = F(T)\exp\{i[k_3 x + m_3 y - \omega_f t + \Theta(T)]\} + cc, \tag{6}$$

where $F(T)$ is the real amplitude of the prescribed external vorticity source, k_3 and m_3 are its zonal and meridional wavenumbers respectively, ω_f is its frequency and a constant, $\Theta(T)$ is an arbitrary slowly varying phase. As pointed out hereafter, the wave three is only forced by the external vorticity source. When $F(T)$ is a constant, the external vorticity source is a constant amplitude forcing, while when $F(T)$ is a slowly varying function, the external vorticity source is a modulated forcing.

In Eq. (4a), if we take $(k_1, m_1) = (k, -2m)$, $(k_2, m_2) = (2k, m)$ and $(k_3, m_3) = (-3k, m)$ as the zonal and meridional wavenumbers of the three Rossby waves for zonal wavenumbers 1–3 considered here (where $k = \dfrac{1}{6.371\cos(\varphi_0)}$ is the zonal wavenumber of the wave one, and $m = \dfrac{\pi}{Ly}$), then when the three Rossby waves in Eq. (4a) satisfy the conditions

$$\vec{K}_1 + \vec{K}_2 + \vec{K}_3 = 0, \quad \omega_1 + \omega_2 + \omega_3 = \Delta\omega, \tag{7}$$

for a small frequency mismatch $\Delta\omega$, three–wave near–resonance among the three Rossby waves may occur (Craik, 1985; Luo, 1994; Luo, 1998). If we choose $Ly = 3 \sim 3.5$, then $\Delta\omega = 0.0634 \sim 0.0365$ at 45°N. In this case, the three–wave near–resonant interaction is permitted. On the other hand, if we assume $\omega_f = \omega_3 + \Delta\omega$ and $\Delta\omega = \varepsilon\Delta\omega_0$ for the small $\Delta\omega$, then by substituting (5) and (6) into Eq. (4b) the nonsecluarity condition requires that

$$\frac{dA_1}{dT} = -R_{e0}A_1 + S_1 A_2^* A_3^* e^{i\Delta\omega_0 T}, \tag{8a}$$

$$\frac{dA_2}{dT} = -R_{e0}A_2 + S_3 A_1^* A_3^* e^{i\Delta\omega_0 T}, \tag{8b}$$

$$\frac{dA_3}{dT} = -R_{e0}A_3 + S_3 A_1^* A_2^* e^{i\Delta\omega_0 T} + F(T)e^{i[-\Delta\omega_0 T + \Theta(T)]}, \tag{8c}$$

where $S_1 = \dfrac{b_1(|K_2|^2 - |K_3|^2)}{|K|^2}$, $S_2 = \dfrac{b_2(|K_3|^2 - |K_1|^2)}{|K_2|^2}$, $S_3 = \dfrac{b_3(|K_1|^2 - |K_2|^2)}{|K_3|^2}$, $b_1 = k_3 m_2 - k_2 m_3$, $b_2 = k_1 m_3 - k_3 m_1$, $b_3 = k_2 m_1 - k_1 m_2$ and A_n^* denotes the complex conjugate of A_n.

When $R_e = 0$, $\Delta\omega_0 = 0$ and $F(T) = 0$, Eqs. (8a–c) reduce to the three–wave resonance equations derived by Longuet–Higgins and Gill (1967), Jones (1979) and Cree and Swaters (1991). However, when $R_e = 0$, $F(T) = 0$, and $\Delta\omega_0 \neq 0$, Eqs. (8a–c) reduce in form to the

three–wave quasi–resonance equations in the geophysical fluid derived by Luo (1994). For cases without forcing and dissipation, the analytic solutions of Eqs. (8a–c) had been obtained by Weiland and Wilhelmsson (1977) and Craik (1985) in terms of Jacobi elliptic functions. In addition, when $F(T)=0$ and R_{e0} in Eq. (8a) is negative, Eqs. (8a–c) are similar to the three–wave coupling model investigated by Wersinger, Finn and Ott(1980a,b), they found that the dynamical behavior of these equations depends strongly on the parameters. In a certain parameter range, the period–doubling bifurcation and chaotic behavior of " strange" attractor were found.

In Eqs. (8a–c), because $S_1<0, S_2<0$ and $S_3<0$, we can make the transformations $A_1=\sqrt{-S_1}B_1, A_2=\sqrt{-S_2}B_2$, and $A_3=\sqrt{S_3}B_3$. In this case, Eqs. (8a–c) can be rewritten as

$$\frac{dB_1}{dT}=-R_{e0}B_1-\chi B_2^* B_3^* e^{i\Delta\omega_0 T}, \tag{9a}$$

$$\frac{dB_2}{dT}=-R_{e0}B_2-\chi B_1^* B_3^* e^{i\Delta\omega_0 T}, \tag{9b}$$

$$\frac{dB_3}{dT}=-R_{e0}B_3+\chi B_1^* B_2^* e^{i\Delta\omega_0 T}+\frac{F(T)}{\sqrt{S_3}}e^{i[-\Delta\omega_0 T+\Theta(T)]}, \tag{9c}$$

where $\chi=\sqrt{S_1S_2S_3}$.

It is clearly found from (9a) and (9b) that B_1 and B_2 have the same equation in the form. If the variables in Eq. (9a–c) have the initial amplitude, then both B_1 and B_2 have the same time variation and identical period. On the other hand, Ghil and Mo (1991) found that in the mid–high latitudes, 30–60–day low frequency oscillations show wavenumber one–through–three nearly equal amplitudes. Based on such observational evidences, we may assume two waves of the three Rossby waves being of equal amplitude. In this case, if we assume $B_1=B_2$ (Wersinger, Finn and Ott 1980 a,b; Hughes and Proctor, 1990a, b, 1992), we obtain from (8a–c)

$$\frac{dB_1}{dT}=-R_{e0}B_1-\chi B_1^* B_3^* e^{i\Delta\omega_0 T}, \tag{10a}$$

$$\frac{dB_3}{dT}=-R_{e0}B_3+\chi B_1^{*2} e^{i\Delta\omega_0 T}+\frac{F(T)}{\sqrt{S_3}}e^{i[-\Delta\omega_0 T+\Theta(T)]}. \tag{10b}$$

Here, we will divide two cases to discuss the dynamical property of equations (10a–b). First, we consider $\Theta(T)=0$. It implies that the external vorticity source is in phase of the wave three. Second, we consider $\Theta(T)\neq 0$. For this case, the external vorticity source has a slowly varying phase difference in comparison with the wave three. On the other hand, it should be pointed out that Eqs. (10a–b) are also different from the two–mode coupling equations derived by Miles (1976) in investigating resonant oscillations of water waves in closed containers subjected to periodic forcing even though $\Delta\omega_0=0$ and $\Theta(T)=0$ are allowed. In the following, we will divide two cases to simplify Eqs. (10a–b).

2.2.1 *The four–variable equations for* $\Theta(T)=0$

In Eqs. (10a–b), if $\Theta(T)=0$, then these equations cannot be reduced to the three–variable equations similar to those derived by Wersinger, Finn and Ott (1980a,b), Hughes and Proctor (1990a,b, 1992), but can be reduced to the four–variable equations. Here, if we assume

$B_1 = b_1(T)e^{i\Delta\omega_0 T}$ and $B_3 = b_3(T)e^{-i\Delta\omega_0 T}$, and define $X(t)= \varepsilon\mathrm{Re}[b_1(\varepsilon t)]$, $Y(t)= \varepsilon\mathrm{Im}[b_1(\varepsilon t)]$, $Z(t)= \varepsilon\mathrm{Re}[b_3(\varepsilon t)]$, and $W(t)= \varepsilon\mathrm{Im}[b_3(\varepsilon t)]$, then the following four-variable equations can be obtained as

$$\frac{dX}{dt} = -R_e X + \Delta\omega Y - \chi(XZ - YW), \tag{11a}$$

$$\frac{dY}{dt} = -R_e Y - \Delta\omega X + \chi(XW - YZ), \tag{11b}$$

$$\frac{dZ}{dt} = -R_e Z - \Delta\omega W + \chi(X^2 - Y^2) + f(t), \tag{11c}$$

$$\frac{dW}{dt} = -R_e W + \Delta\omega Z - 2\chi XY. \tag{11d}$$

In Eqs. (11a–d), if $f(t)$ is a constant, then the stability analysis of these equations can be made. As an example, for Eqs. (11a–d) we only consider the $f(t)=$constant case. Thus, we may assume $f(t)= f_0$ (f_0 is a constant). Moreover, the stability analysis of system (11) will be discussed in Section 3, and its chaotic solutions are also given.

2.2.2 *The reduced three-variable equations for* $\Theta(T)\neq 0$

In Eqs. (10a–b), when $\Theta(T)\neq 0$, the external vorticity source has a slowly varying phase difference in comparison with the wave three. Here, if $B_1(T)= r_1(T)e^{i[\Delta\omega_0 T+\varphi_1(T)]}$ and $B_3(T) = r_3(T)e^{i[-\Delta\omega_0 T+\varphi_3(T)]}$ are allowed, then $\Theta(T)$ may be assumed to satisfy $\Theta(T)= -2\varphi_1(T)$. In this case, if one uses $t= T/\varepsilon$ and defines

$$X(t)= \varepsilon r_3(T)\cos\Phi,\ Y(t)= \varepsilon r_3(T)\sin\Phi,\ Z(t)= \varepsilon^2 r_1(T)^2 \tag{12}$$

for $\Phi= -2\varphi_1(T)-\varphi_3(T)$, then we obtain from Eqs. (10a–b)

$$\frac{dX}{dt} = -R_e X - \Delta\omega Y + \chi Z - 2\chi Y^2 + f(t), \tag{13a}$$

$$\frac{dY}{dt} = -R_e Y + \Delta\omega X + 2\chi XY, \tag{13b}$$

$$\frac{dZ}{dt} = -2Z(R_e + \chi X), \tag{13c}$$

where $R_e = \varepsilon R_{e0}$, $\Delta\omega= \varepsilon_0\Delta\omega$ and $f(t)= \dfrac{\varepsilon^2 F(\varepsilon t)}{\sqrt{S_3}}$.

When $f(t)= 0$, and only when R_e and $\Delta\omega$ in Eqs. (13a–b) are replaced by $-R_e$ and $-\Delta\omega$ respectively, Eqs. (13a–c) are identical in form to the three-variable nonlinear equations in the conext of waves in plasmas derived by Wersinger, Finn and Ott (1980a, b), Hughes and Proctor (1990a, b, 1992), who investigated in detail the bifurcation and chaotic behavior of this system. Hughes and Proctor (1990b) reduced these equations to a one-dimensional, bimodal map of successive maxima of $|X|$, and found that the dynamics of these equations can be described in terms of the bimodal one-dimensional map, which allows bifurcation sequences etc. to be simply constructed. On the other hand, when $f(t)\neq 0$, Eqs. (13a–c) obtained here are new forced three-variable nonlinear equations, which has not been investigated yet. In this paper, we will apply the fourth-order Rung-Kutta method to solving Eqs. (13a–c). In fact, because R_e is always positive in the large-scale flow, these equations

may have different properties in comparison with the three-variable equations obtained by Hughes and Proctor (1990b). If we define $E = X^2 + Y^2 + Z$, then $\frac{dE}{dt} = -2R_e E + 2f(t)X$. In this case, the total energy E of the three coupling waves is not a conserved quantity. This indicates that the dynamical behavior of the three coupling waves is rather complex.

3. The stability analysis without dissipation and numerical solution of system (11) under the constant amplitude forcing

3.1 *The stability analysis without dissipation and pitchfork bifurcation*

In this section, the stability analysis of system (11) is made. For simplicity, we consider the inviscid case. When $f_0 > 0 (f(t) = f_0)$, by setting $R_e = 0$ and $\frac{dX}{dt} = \frac{dy}{dt} = \frac{dZ}{dt} = \frac{dW}{dt} = 0$, three stationary solutions of Eqs. (10a–d) are easily obtained; with $P = (X,Y,Z,W)$, they are

$$P_0 = (0,0,0,\frac{f_0}{\Delta\omega}),\ P_{1,2} = (0,\pm\sqrt{\frac{(\Delta\omega^2 + f_0\delta)}{\delta^2}},0,-\frac{\Delta\omega}{\delta}). \tag{14}$$

When $f_0 < 0$, the three stationary solutions of Eqs. (11a–d) are

$$P_0 = (0,0,0,\frac{f_0}{\Delta\omega}),\ P_{1,2} = (\pm\sqrt{\frac{(\Delta\omega^2 - f_0\delta)}{\delta^2}},0,0,\frac{\Delta\omega}{\delta}). \tag{15}$$

In order to investigate the stability of the stationary solutions, we linearize Eqs. (11a–d) by $P' = P - P_i (i = 0,1,2)$ to yield

$$\dot{P}' = \begin{bmatrix} 0 & \Delta\omega + \delta W_i & 0 & \delta Y_i \\ -(\Delta\omega - \delta W_i) & 0 & \delta Y_i & 0 \\ 0 & -2\delta Y_i & 0 & -\Delta\omega \\ -2\delta Y_i & 0 & \Delta\omega & 0 \end{bmatrix} P',\ i = 0,1,2, \tag{16}$$

for $f_0 > 0$, where $P' = \begin{bmatrix} X' \\ Y' \\ Z' \\ W' \end{bmatrix}$.

For the stationary solution P_0, the characteristic equation of systems (11a–d) without dissipation is

$$(\lambda^2 + \Delta\omega^2)(\lambda^2 + \Delta\omega^2 - \frac{\delta^2 f_0^2}{\Delta\omega^2}) = 0, \tag{17}$$

but for the stationary solutions $P_{1,2}$, their eigenvalue equation is

$$\lambda^4 + \lambda^2[\Delta\omega^2 + 4(\Delta\omega^2 + f_0\delta)] + 4(\Delta\omega^2 + f_0\delta)f_0\delta = 0 \tag{18}$$

When $f_0^2 < \frac{\Delta\omega^4}{\delta^2}$, Eq. (17) has four imaginary roots. In this case, the stationary

solution P_0 is stable. While when $f_0^2 > \frac{\Delta\omega^4}{\delta^2}$, Eq. (17) has four imaginary roots. In this case, the stationary solution P_0 is unstable. On the other hand, it is found that Eq. (18) only has four imaginary roots. This shows that simultaneous with the loss of the stability of P_0, the stable two fixed points P_1 and P_2 are born. Thus, as f_0 increase through $\frac{|\Delta\omega|^2}{\delta}$, P_1 and P_2 become the attractors of the system. The basin boundary separating the basins of attraction for the attractors P_1 and P_2 is the two-dimensional stable manifold of P_0 (Jackson, 1990, and Ott, 1993). For $f_0 < 0$, there exists similar pitchfork bifurcation. Thus, when $|f_0|$ increases, a pitchfork bifurcation will occur (Guckenheimer and Holmes, 1986). In next subsection, we will find numerically that the pitchfork bifurcation can lead to chaotic solutions.

3.2 *Numerical results*

3.2.1 *Case* $f_0 > 0$

For the constant f_0 case, we will give the numerical results of systems (11a–d). Without the loss of generality, if we choose the initial data $X(0) = Y(0) = Z(0) = W(0) = 0.3$ and $R_e = 0.0001$, then under the condition $f_0 > 0$, the fourth-order Rung-Kutta scheme may be applied to computing systems (11a–d) for the given f_0. For $f_0 = 0.02, 0.074, 0.11, 0.16, 0.18$ and 0.20, the projections onto the (X,Y)-plane of trajectories of systems (10a–d) are shown in Fig. 1, while the corresponding time evolution solutions for X of systems (11a–d) are described in Fig. 2.

It is found from systems (11a–d) that under $(X,Y,Z,W) = (-X,-Y,Z,W)$, system (11) possesses invariance. This character is consistent with that found in the Lorenz system. As pointed out by the stability analysis of the fixed points of system (11), carried out in the above subsection, when the parameter f_0 increases, the pitchfork bifurcation occurs and produces an interesting arrangement of limit cycles. The limit cycle, which is invariant under $(X,Y,Z,W) = (-X,-Y,Z,W)$, becomes unstable and two stable limit cycles are formed. We see in Figure 1 that when $f_0 = 0.02$, the phase trajectory in the (X,Y)-plane for the solutions of system (11) is a symmetric period-two orbit, and its main period is near 40 days. While when $f_0 = 0.074$, a period-three orbit is observed through the bifurcation. As f_0 increases further, chaotic motions can occur through the pitchfork bifurcation. For example, when $f_0 = 0.11, 0.16, 0.18$ and 2.0, the solutions of $X(t)$ are found to possess chaotic behavior, while the corresponding phase trajectories are found to be strange attractors that seem to have "inkfish", "dragofly", "petal" et al. patterns. Interestingly, it can be noted that these strange attractors found in Figs. 1c–f are symmetric in the X direction. Thus, the pitchfork bifurcation can lead to chaos as f_0 is increased. Although system (11) is a new chaotic model, its symmetry is found to be the same as the Lorenz system. In system (11), the pitchfork bifurcation is only observed, while in the Lorenz system subcritical Hopf bifurcation can be found except the pitchfork bifurcation. For the Lorenz system, the onset route of chaos was given in detail in Sparrow (1982) and Drazin (1993). Here, for system (11) we only give the numerical result of chaos onset. Interestingly, we note that with the variation of the parameter f_0 in the range from 0.02 to 0.2, the dominant period of X varies from 50 days to 80 days, which belongs to low-frequency period band (Luo, 1997).

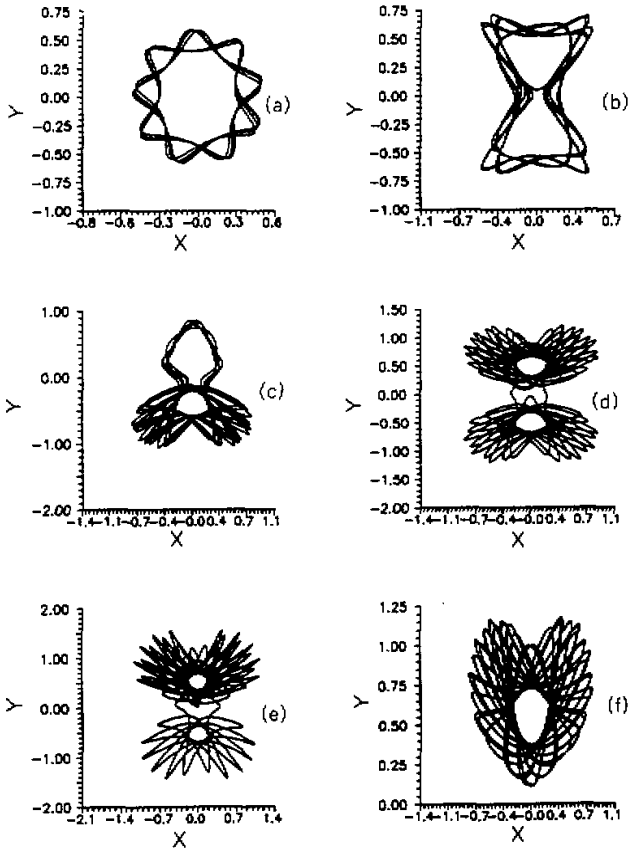

Fig. 1. Projections onto the (X,Y) plane of trajectories of system (11): (a) $f_0 = 0.02$, (b) $f_0 = 0.074$, (c) $f_0 = 0.11$, (d) $f_0 = 0.16$, (e) $f_0 = 0.18$, (f) $f_0 = 0.20$.

3.2.2 *Case* $f_0 < 0$

For $f_0 < 0$, if we choose $f_0 = -0.0162$, -0.031, -0.04, -0.07, -0.16 and -0.18, then under the same conditions as in Fig. 1 the projections onto the (X,Y)–plane of trajectories of system (11) and evolution of $X(t)$ are shown in Figs. 3 and 4, respectively.

It is found from Fig. 3 that when $f_0 = -0.0162$, the phase trajectory in the (X,Y)–plane for the solutions of system (11) looks like a sunflower, which seems to be a period–two orbit. In fact, we note from the evolution of $X(t)$ in Fig. 4 that when $f_0 = -0.0162$, $X(t)$ is approximately a periodic solution. When f_0 decreases, a period–doubling bifurcation is observed. For example, when $f_0 = -0.04$, a quadruple–period limit cycle is observed in Fig. 3c. However, as f_0 decreases further, the period–doubling cascade can lead to chaotic solutions (Drazin, 1993). For example, when $f_0 = -0.07$, -0.16 and -0.18 the phase portraits in Figs. 4d–f are found to be strange attractors that look like the "petal" pattern. This shows that the

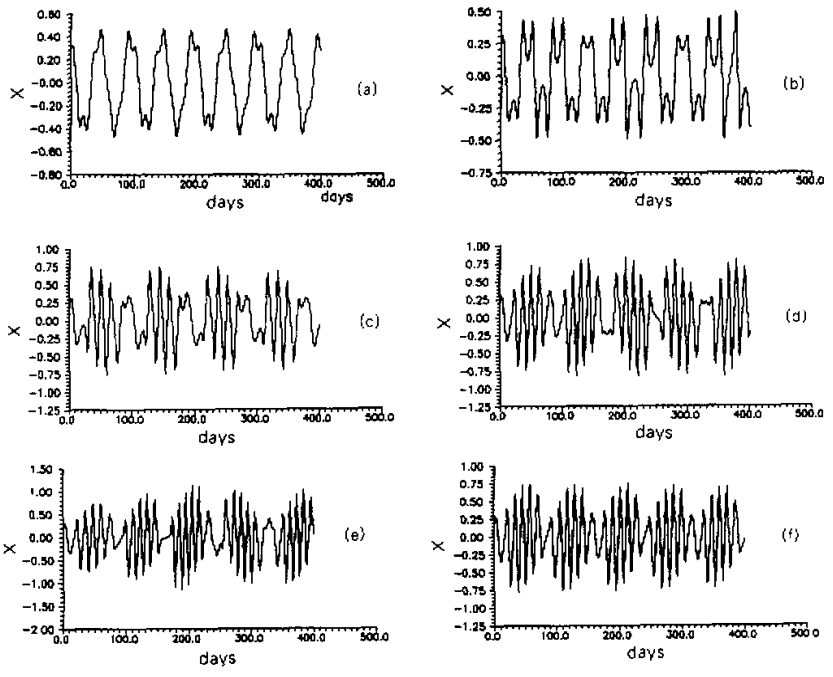

Fig. 2. Evolution of $X(t)$ for the solutions in Figs. 1a–f: (a) $f_0 = 0.02$, (b) $f_0 = 0.074$, (c) $f_0 = 0.11$, (d) $f_0 = 0.16$, (e) $f_0 = 0.18$, (f) $f_0 = 0.20$.

strange attractor pattern depends on the sign of f_0. Different from Figs. 1c–f, these strange attractors are symmetric in the Y direction. On the other hand, by observing the evolution of $X(t)$ we find that the solution of $X(t)$ is a chaotic solution when $f_0 = -0.07 \sim -0.18$. Thus, chaos can occur through the pitchfork bifurcation in system (11) as f_0 reaches a certain extent for $f_0 < 0$.

In the chaotic three–wave coupling models without forcing proposed by Wersinger, Finn and Ott (1980a,b) and Hughes and Proctor (1990a,b,1992), they assumed that one wave is linearly unstable and the other two are linearly damped. In such a system, the "chaotic" behavior of a "strange" attractor was detected. However, if the three waves are linearly damped, and the external forcing is excluded, no chaotic behavior can be found. In the real atmosphere, all Rossby waves are linearly damped if the dissipation is included. Thus, their obtained model cannot describe nonlinear three–wave coupling among Rossby waves in the large–scale forced barotropic flow. In this case, it is necessary to re–establish a new nonlinear three–wave coupling model. It should be pointed out that if the dissipation is very strong, only decay solutions can be found in system (11). For example, when $R_e = 0.1$, all solutions of system (11) tend to reach stationary state (figures omitted). In addition, we note that in the nonlinear three–wave coupling model, if the external forcing is included, in the general case the coupling model cannot be directly reduced to the three–variable equations. Only under a special condition the coupling model can be reduced to the three–variable equations derived by Wersinger, Finn and Ott (1980a,b) and Hughes and Proctor (1990a,b, 1992). For example,

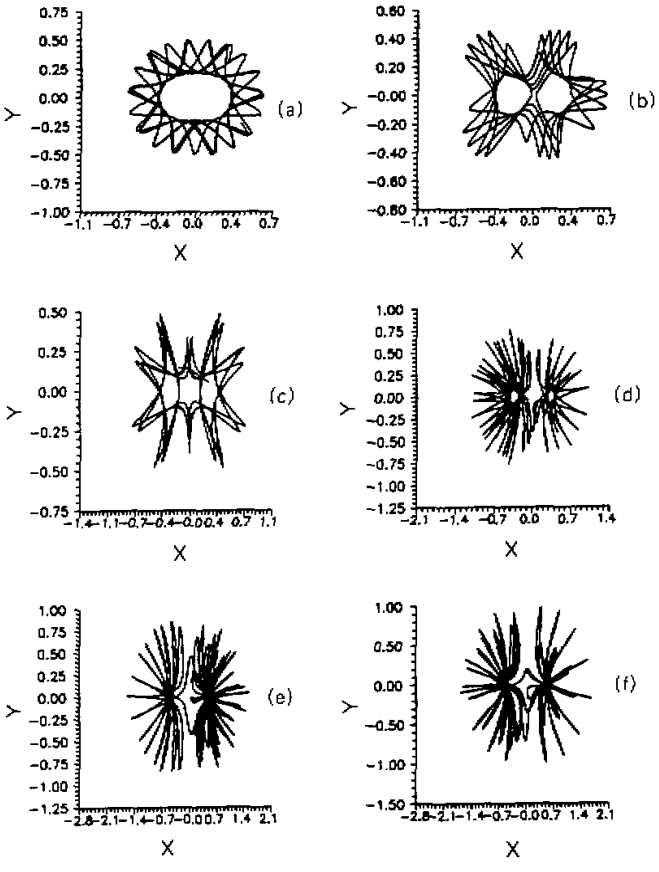

Fig. 3. Projections onto the (X,Y)-plane of trajectories of system (11): (a) $f_0 = -0.0162$, (b) $f_0 = -0.031$, (c) $f_0 = -0.04$, (d) $f_0 = -0.07$, (e) $f_0 = -0.16$, (f) $f_0 = -0.18$.

when $\Theta(T) = 0$ the forced coupling model like Eqs. (8a–c) can be reduced to the four-variable equations such as system (11). While when $\Theta(T) = -2\varphi_1(T)$, the forced coupling model can be changed into the three-variable equations. In this section, the numerical study of system (11) indicates that if the external forcing is considered, chaos can also occur though the three waves are linearly damped. In the next section, we will investigate whether chaos can occur in system (13).

4. Numerical result of system (13) under a modulated forcing with weak dissipation ($R_e = 0.0001$)

In system (13), the external forcing $f(t)$ is assumed to be of the form $f(t) = f_0 + f_1 \cos\Omega t$, where Ω is the frequency of the prescribed modulated external vorticity source. In the

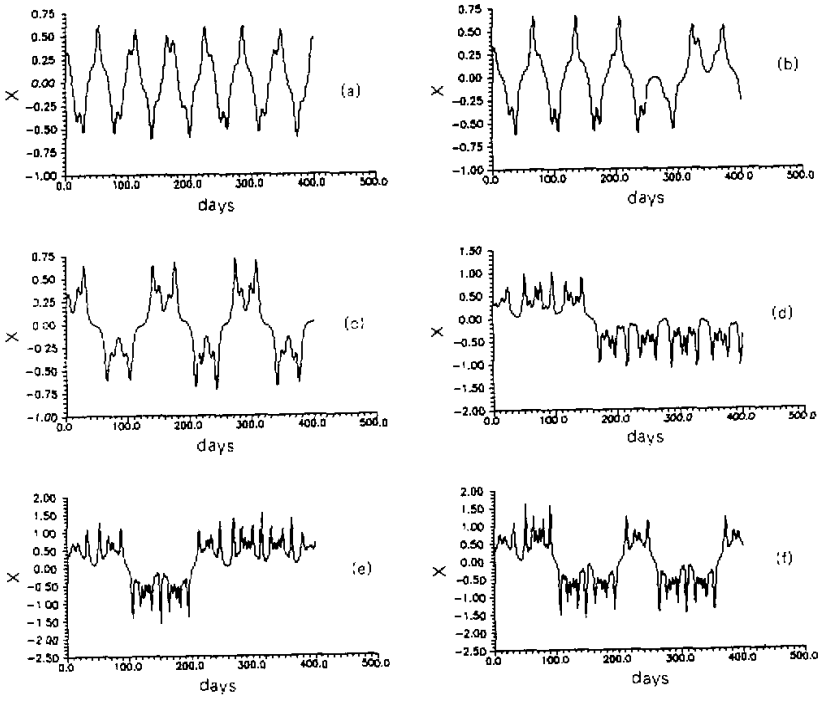

Fig. 4. Evolution of $X(t)$ for the solutions in Figs. 3a–f: (a) $f_0=-0.0162$, (b) $f_0=-0.031$, (c) $f_0=-0.04$, (d) $f_0=-0.07$, (e) $f_0=-0.16$, (f) $f_0=-0.18$.

Northern Hemispheric mid–high latitudes, Lau and Holopainen (1984) had shown that the period of the net forcing due to transient eddies is longer than ~ 7–10 days but less than a season (~ 90 days). Usually the period of the large–scale transient forcing is chosen to be about 20 days. Here if the transient eddy vorticity forcing is considered as an external vorticity source, the period of the external forcing $f(t)$ may be chosen to be 20 days, i.e., $\Omega=0.361$. If we choose the initial data $X(0)=Y(0)=Z(0)=0.1$ and $R_e=0.0001$, then for $f_0=0.02$ the phase portrait in the (X,Y)–plane for the solutions of system (13) and the time evolution of $X(t)$ for different f_1 are shown in Figs. 5 and 6, respectively.

It can be seen from Figs. 5 and 6 that for $f_0=0.02$, when $f_1=0.0$, the phase protrait in the (X,Y)–plane for the solutions of system (13) is a period–one limit cycle, and the solution $X(t)$ possesses a nearly 16–day period. When $f_1=0.0124$, a double–period limit cycle appears, and a long periodic oscillation is observed, which can be found from Figs. 5b and 6b. As f_1 continues to increrase, further bifurcation can be detected. For example, when $f_1=0.087$ a triple–period limit cycle is found in Fig. 5c. For this case, the main period of the solution $X(t)$ is near 40 days, which is within the range of 30–60–day period. When f_1 increases further, the chaotic solutions of system (13) can be found. For example, when f_1 increases from 0.0425 to 0.92, chaos appears. Figs. 5e–f describe two "strange" attractors at $f_1=0.54$ and 0.92. Moreover, under these conditions $X(t)$ is a clearly chaotic solution. Thus, for perscribed modulated external forcing, when its modulated amplitude reaches a certain extent, chaos can occur through a series of period–doubling bifurcation. Unfornately,

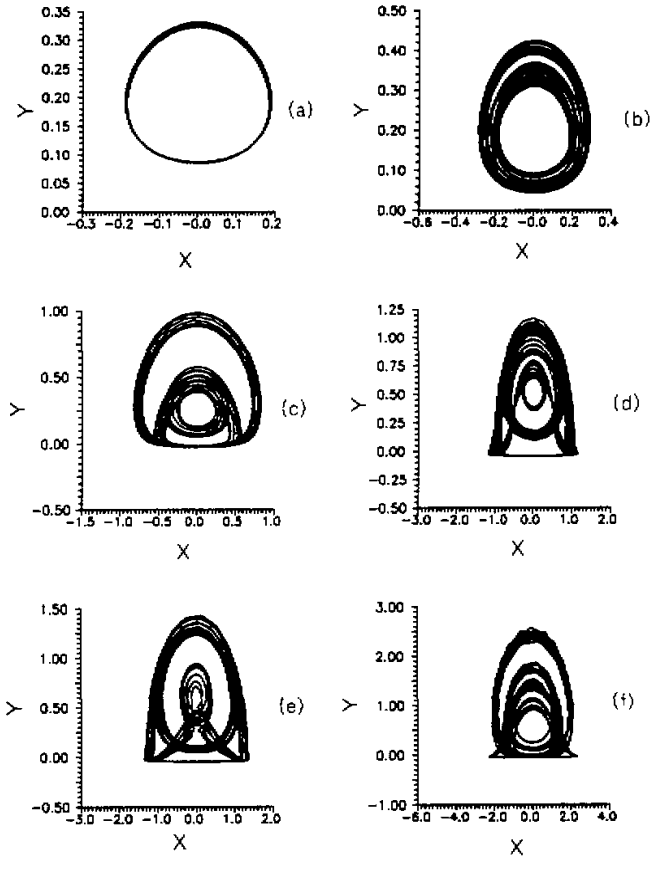

Fig. 5. The phase portrait in the (X,Y)–plane for the solutions of system (13): (a) $f_1 = 0.0$, (b) $f_1 = 0.0124$, (c) $f_1 = 0.087$, (d) $f_1 = 0.425$, (e) $f_1 = 0.54$, (f) $f_1 = 0.92$.

when $f_1 = 0.0$, no chaos can be detected even if f_0 is arbitrarily chosen. Consequently, when the modulated amplitude of forcing increases, 30–60–day low–freqeuncy oscillation can be excited through period–doubling bifurcation.

5. Numerical result of system (13) under a modulated forcing with stronger dissipation ($R_e = 0.1$)

Under the same condition, if we consider stronger dissipation (for example, $R_e = 0.1$), then the phase portrait in the (X,Y)–plane for the solutions of system (13) and the time evolution of $X(t)$ for different f_1 are shown in Figs. 7 and 8, respectively.

It is found from Fig. 8 that for $R_e = 0.1$ when $f_1 = 0.0$, the solution of system (13) becomes stationary state solution. However, when f_1 gradually increases, the solution of this

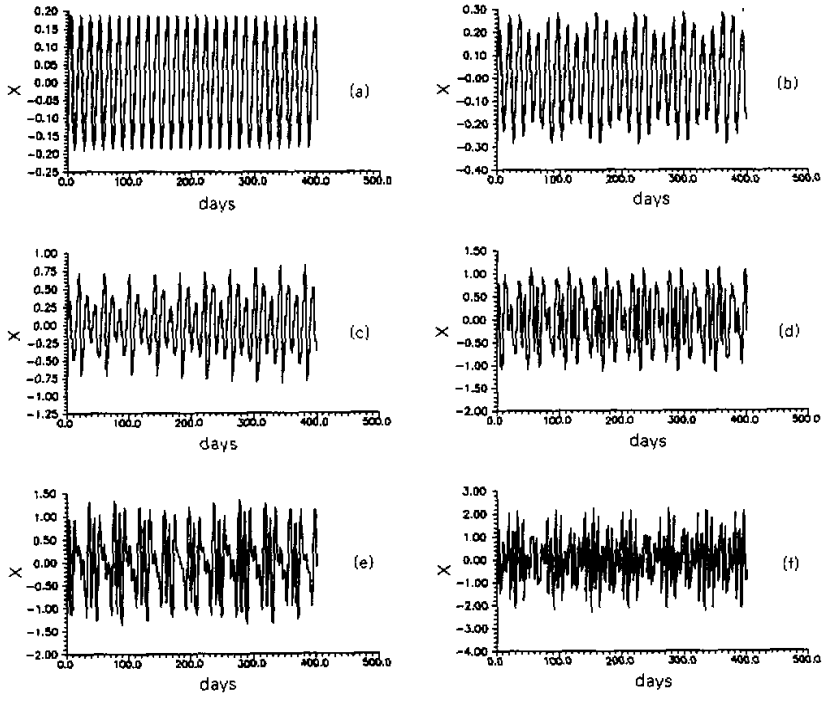

Fig. 6. Evolution of $X(t)$ for the solutions in Figs. 5a–f: (a) $f_1 = 0.0$, (b) $f_1 = 0.0124$, (c) $f_1 = 0.087$, (d) $f_1 = 0.425$, (e) $f_1 = 0.54$, (f) $f_1 = 0.92$.

system becomes oscillatory ones. In a certain parameter range, this solution may be aperiodic. Unfortunately, the long aperiod of this solution is not longer than that in Fig. 7. On the other hand, the comparison between Figs.5 and 7 indicates that the dissipation does also have an important influence on the phase portrait. Thus, only in a moderate dissipation parameter range, long periodic oscillation and chaotic motion can be observed.

In the geophysical fluid, nonlinear three–wave coupling among Rossby waves in large–scale free or forced barotropic and baroclinic flows had been investigated in detail by many investigators such as Longuet–Higgins and Gill (1967), Jones (1979), Cree and Swaters (1991), Luo (1994) and Luo (1998), some results were obtained. But, unfortunately, no chaos was found. Here, for the forced three–variable equations obtained, when the parameters reach a certain extent, this sytem can exhibit chaotic behavior. Thus, the forced three–variable equations obtained here may be considered as the generalization of the three–variable equations derived by Hughes and Proctor (1990b).

6. Conclusions

In this paper, new chaotic models describing nonlinear three–wave interaction among Rossby waves in a large–scale forced barotropic flow are obtained. In the reduced four–variable model, a pitchfork bifurcation occurs and leads to chaos when the prescribed external vorticity source is a constant amplitude forcing and gradually increases. For the reduced

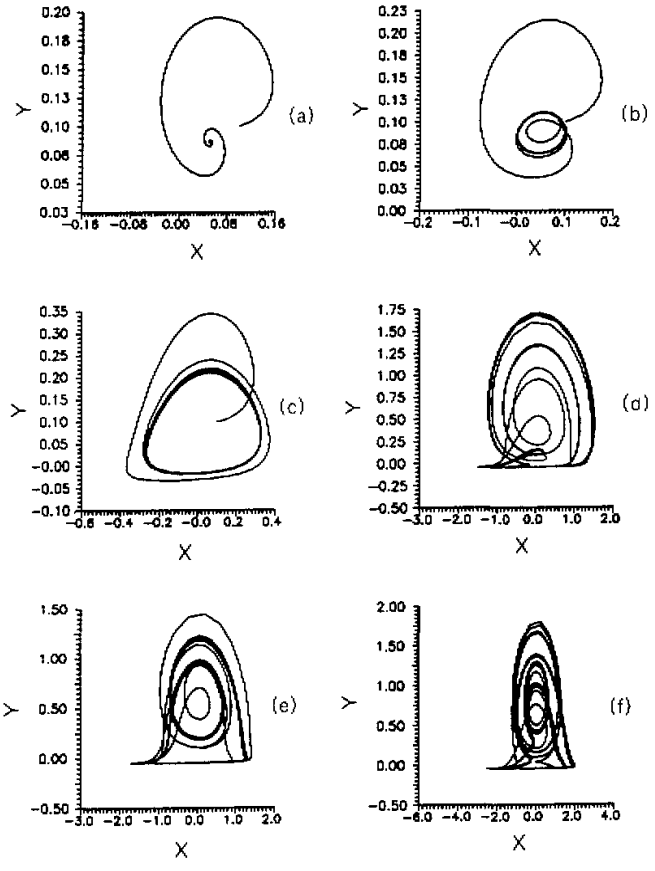

Fig. 7. The phase portrait in the (X,Y)-plane for the solutions of system (13) with stronger dissipation ($R_e = 0.1$).(a) $f_1 = 0.0$, (b) $f_1 = 0.0124$, (c) $f_1 = 0.087$, (d) $f_1 = 0.425$, (e) $f_1 = 0.54$, (f) $f_1 = 0.92$.

three-variable model, it is found from numerical results that chaos can occur through a series of period-doubling bifurcation when the prescribed external vorticity source is a modulated forcing and the modulated amplitude increases. These chaotic behaviors can explain in part the aperiodicity of 30-60-day low-frequency oscillation. Certainly, if the prescribed external vorticity source has different form, the obtained conclusion may be different. On the other hand, the dissipation has an important influence on the model behavior.

Although chaotic behavior of new "strange" attractor is found in this paper further work on this subject needs to be carried out in the future.

This work has been sponsored by the Sichuan Youth Science and Technology Foundation.

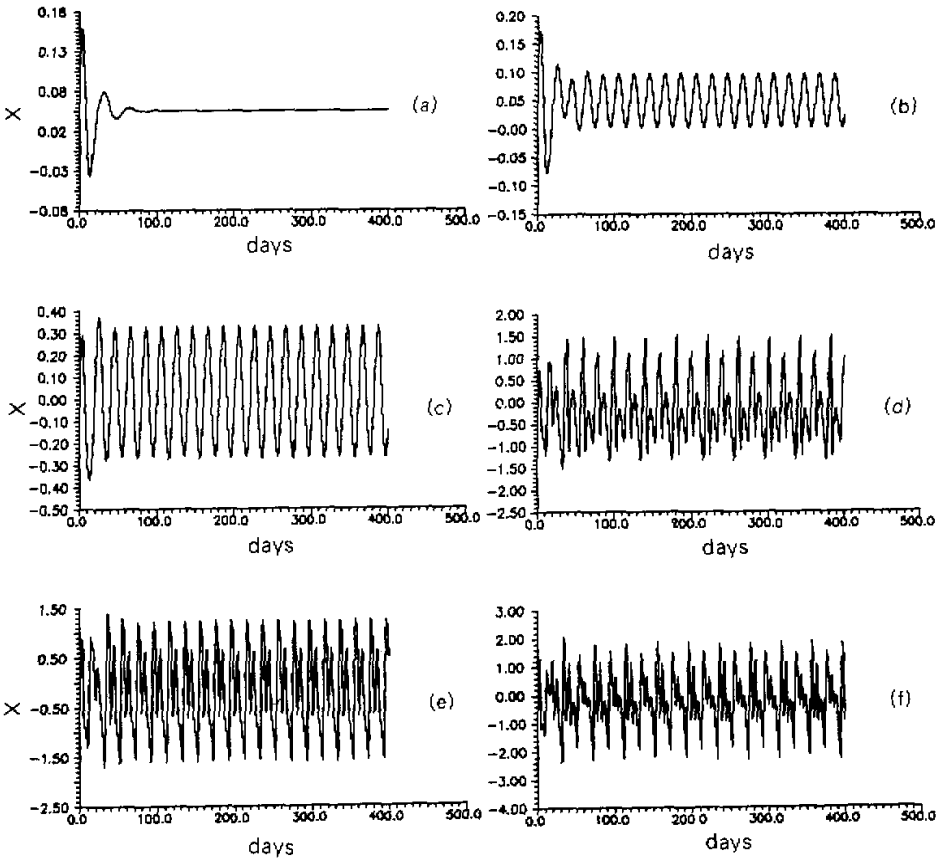

Fig. 8. Evolution of $X(t)$ for the solutions in Figs. 7a–f: (a) $f_1 = 0.0$, (b) $f_1 = 0.0124$, (c) $f_1 = 0.087$, (d) $f_1 = 0.425$, (e) $f_1 = 0.54$, (f) $f_1 = 0.92$.

REFERENCES

Charney, J. G., and Devore, J. G., 1979: Multiple equilibria in the atmosphere and blocking. *J. Atmos. Sci.*, **36**, 1205–1216.

Craik, A. D. D., 1985: *Wave Interactions and Fluid Flows.* Cambridge University Press 360 pp.

Cree, W. C., and Swaters, G. E., 1991: On the topographic dephasing and amplitude modulation of nonlinear Rossby wave interaction. *Geophys. Astrophys. Fluid, Dyn.*, **61**, 75–99.

Drazin, P. G., 1993: *Nonlinear systems.* Cambridge University Press 317 pp.

Egger, J., 1978: Dynamics of blocking high. *J. Atmos. Sci.*, **35**, 1788–1801.

Guckenheimer, J. and Holmes, P. J., 1986: *Nonlinear oscillations, Dynamical systems and Bifurcations of Vector fields*, 2nd edition, New York, Springer–Verlag. *Appl. Math. Sci.*, **42**.

Ghil, M., and Mo K., 1991: Intraseasonal oscillations in the Global atmosphere. Part I: Northern Hemisphere and tropics, *J. Atmos. Sci.*, **48**, 752–790.

Hughes, D. W., and Proctor, M. R. E., 1990a: Chaos and the effect of noise in a model of three-wave mode coupling. *Physica*, **D46**, 163–176.

Hughes, D. W., and Proctor, M. R. E. 1990b: A low-order model for the shear instability for convection: Chaos and the effect of noise, *Nonlinearity*, **3**, 127–153.

Hughes, D. W., and Proctor, M. R. E., 1992: Nonlinear three-wave interaction with non-conservative coupling. *J. Fluid Mech.*, **244**, 583–604.

Jackson, E. A., 1990: *Perspectives of nonlinear dynamics*. Cambridge University Press 447 pp.

Jones, S., 1979: Rossby wave interactions and instabilities in a rotating, two layer fluid on a beta-plane. Part I: Resonant interactions. *Geophys. Astrophys. Fluid, Dyn.*, **11**, 289–322.

Lau, N. C., and Holopainen, E. O., 1984: Transient eddy forcing of the time-mean flow as identified by geopotential tendencies. *J. Atmos. Sci.*, **41**, 313–328.

Loesch, A. Z., 1974: Resonant interactions between unstable and neutral baroclinic waves. Part I. *J. Atmos. Sci.*, **31**, 1177–1201.

Longuet-Higgins, M. S., and Gill, A. E., 1967: Resonant interactions between planetary waves. *Proc. R. Soc. Lond.*, **A229**, 120–140.

Lorenz, E. N., 1963: Deterministic nonperiodic flow. *J. Atmos. Sci.*, **20**, 130–141.

Luo, D. H., 1994: Quasi-resonant interactions among barotropic Rossby waves with two-wave topography and low frequency dynamics. *Geophys. Astrophys. Fluid Dyn.*, **76**, 145–163.

Luo, D. H., 1997: Low frequency finite-amplitude oscillations in a near resonant topographically forced barotropic flow. *Dyn. Atmos. Oceans*, **26**, 53–72.

Luo, D. H., 1998: Topographically forced three-wave quasi-resonant and non-resonant interactions among barotropic Rossby waves on an infinite beta-plane. *Adv. Atmos. Sci.*, **15**, 83–98.

Miles, J. W., 1976: On the internal resonance of two damped oscillators. *Stud. Appl. Math.*, **55**, 351–359.

Ott, E., 1993: *Chaos in dyamical systems*. Cambridge University Press 304 pp.

Sparrow, C., 1982: *The Lorenz Equations, Bifurcations, Chaos, and Strange Attractors*, New York: Springer-Verlag. *App. Math. Sci.*, **41**.

Weiland, J., and Wilhelmsson, H., 1977: Coherent nonlinear interaction of waves in Plasmas. Oxford, Pergamon 297 pp.

Wersinger, J. M., Finn, J. M., and Ott, E., 1980a: Bifurcations and strange behavior in instability saturation by nonlinear mode coupling. *Phys. Rev. Lett.*, **44**, 453–456.

Wersinger, J. M., Finn, J. M., and Ott, E., 1980b: Bifurcations and strange behavior in instability saturation by nonlinear three wave mode coupling. *Phys. Fluids.*, **23**, 1142–1154.